

ANALYSIS OF H-PLANE WAVEGUIDE JUNCTION WITH DIELECTRIC COATED FERRITE CYLINDER BY MODE MATCHING METHOD

Akira MATSUSHIMA and Daisuke MURASATO

Department of Electrical and Computer Science, Kumamoto University
 2-39-1 Kurokami, Kumamoto 860-8555 Japan
 E-mail: matsua@eecs.kumamoto-u.ac.jp

Abstract The H-plane Y-junction circulator of rectangular waveguides is analyzed by the mode matching method. This technique can easily treat the case where the ferrite cylinder is coated by dielectric material and their cross sections are deformed from circles. We discuss the frequency characteristics of the circulator and demonstrate that the dielectric coating widens the practical frequency band.

1. INTRODUCTION

The characteristics of the H-plane Y-junction circulator of a rectangular waveguides have been analyzed by a lot of numerical techniques [1–5]. Though the ferrite cylinder with circular cross section has been mainly treated [1,2,5], we cannot obtain sufficiently wide frequency band by such a simple structure. The ways to overcome this difficulty is to perform the impedance matching by deforming the ferrite shape to a triangle [3,4] or by coating the ferrite by dielectric material [6]. But these means work poor if the cross section is not optimized [2].

From this viewpoint, we consider the case where the cross sections of both ferrite and dielectric media are deformed from circles. The mode matching method based on the least squares [7] is used. The cross sections of the cylinders are expressed by Fourier series. After the error in the numerical treatment is examined, the properties the circulator, i.e., the reflection, insertion, and isolation losses are demonstrated for several cross section shapes. The effect of dielectric coating is discussed. The time dependence is assumed to be $e^{j\omega t}$ and will be suppressed throughout.

2. ELECTROMAGNETIC FIELDS

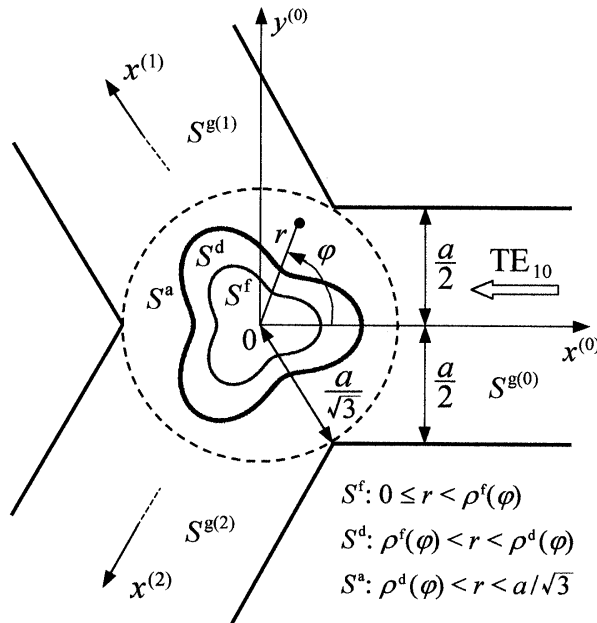


Figure 1: Geometry of the problem.

Figure 1 shows the H-plane Y-junction of the rectangular waveguides having the $2\pi/3$ -rotational symmetry. The $x^{(u)}$ -axis ($u = 0, 1, 2$) is set parallel to the wall of the waveguide region $S^{g(u)}$. The circular junction part is composed of the ferrite, dielectric, and air regions, denoted by S^f , S^d , and S^a , respectively. The contour of $S^{f,d}$ is expressed by $r = \rho^{f,d}(\varphi)$ ($0 \leq \varphi < 2\pi$). The permittivity is ϵ , ϵ_1 , and ϵ_0 in the region S^f , S^d , and $S^a \cup S^{g(u)}$, respectively. The permeability in S^f is

the tensor $\begin{bmatrix} \mu & -j\kappa & 0 \\ j\kappa & \mu & 0 \\ 0 & 0 & \mu_0 \end{bmatrix}$, while in the other regions it equals μ_0 .

When the TE_{10} mode is incident from the waveguide (0), the scattered field in each waveguide is expressed by the sum of the TE_{q0} modes. They are written as

$$\begin{cases} E_z^i(x^{(0)}, y^{(0)}) = \sin \left[\pi \left(\frac{1}{2} + \frac{y^{(0)}}{a} \right) \right] e^{\Gamma_1(x^{(0)} - a/2\sqrt{3})} \\ E_z^{g(u)}(x^{(u)}, y^{(u)}) = \sum_{q=1}^{\infty} B_q^{(u)} \sin \left[q\pi \left(\frac{1}{2} + \frac{y^{(u)}}{a} \right) \right] e^{-\Gamma_q(x^{(u)} - a/2\sqrt{3})} \end{cases} \quad (1)$$

where $\Gamma_q = [(q\pi/a)^2 - k_0^2]^{1/2}$ ($\text{Im} \Gamma_q \geq 0$), $k_0 = \omega\sqrt{\varepsilon_0\mu_0}$. The magnetic field has only x and y components and is derived from Maxwell's equations. The electric field in the junction part is

$$\begin{cases} E_z^f(r, \varphi) = \sum_{n=-\infty}^{\infty} A_n J_n(kr) e^{jn\varphi}, & E_z^d(r, \varphi) = \sum_{n=-\infty}^{\infty} [F_n J_n(k_1 r) + G_n Y_n(k_1 r)] e^{jn\varphi} \\ E_z^a(r, \varphi) = \sum_{n=-\infty}^{\infty} [C_n J_n(k_0 r) + D_n Y_n(k_0 r)] e^{jn\varphi} \end{cases} \quad (2)$$

where $k = \omega\sqrt{\varepsilon\mu(1 - \kappa^2/\mu^2)}$, $k_1 = \omega\sqrt{\varepsilon_1\mu_0}$. The magnetic field has only r and φ components.

3. MODE MATCHING METHOD

Truncating the tangential fields on the boundaries by a finite number of terms, we make the approximate wave functions E_N^f , H_N^f , \dots , $H_Q^{g(u)}$ for $0 \leq \varphi < 2\pi$ as ($\zeta_0 = \sqrt{\mu_0/\varepsilon_0}$)

$$\zeta_0 H_{\tan}^f \Big|_{r=\rho^f(\varphi)} \approx E_N^f \Big|_{r=\rho^f(\varphi)} = \sum_{n=-3N}^{3N} A_n \frac{e_n^f}{h_n^f}(\varphi) \quad (3)$$

$$\zeta_0 H_{\tan}^d \Big|_{r=\rho^d(\varphi)} \approx E_N^{d-} \Big|_{r=\rho^d(\varphi)} = \sum_{n=-3N}^{3N} \left[F_n \frac{e_n^{d1}}{h_n^{d1}}(\varphi) + G_n \frac{e_n^{d2}}{h_n^{d2}}(\varphi) \right] \quad (4)$$

$$\zeta_0 H_{\tan}^d \Big|_{r=\rho^d(\varphi)} \approx E_N^{d+} \Big|_{r=\rho^d(\varphi)} = \sum_{n=-3N}^{3N} \left[F_n \frac{e_n^{d3}}{h_n^{d3}}(\varphi) + G_n \frac{e_n^{d4}}{h_n^{d4}}(\varphi) \right] \quad (5)$$

$$\zeta_0 H_{\tan}^a \Big|_{r=\rho^d(\varphi)} \approx E_N^{a-} \Big|_{r=\rho^d(\varphi)} = \sum_{n=-3N}^{3N} \left[C_n \frac{e_n^{a1}}{h_n^{a1}}(\varphi) + D_n \frac{e_n^{a2}}{h_n^{a2}}(\varphi) \right] \quad (6)$$

$$\zeta_0 H_{\tan}^a \Big|_{r=a/\sqrt{3}} \approx E_N^{a+} \Big|_{r=a/\sqrt{3}} = \sum_{n=-3N}^{3N} \left[C_n \frac{e_n^{a3}}{h_n^{a3}}(\varphi) + D_n \frac{e_n^{a4}}{h_n^{a4}}(\varphi) \right] \quad (7)$$

$$\zeta_0 H_{\tan}^{g(u)} \Big|_{r=a/\sqrt{3}, \varphi \rightarrow \varphi_0^{(u)} + \varphi} \approx E_Q^{g(u)} \Big|_{r=a/\sqrt{3}, \varphi \rightarrow \varphi_0^{(u)} + \varphi} = \sum_{q=1}^Q B_q^{(u)} \frac{e_q^g}{h_q^g}(\varphi) \quad \left(\varphi_0^{(u)} = \frac{2u\pi}{3} \right) \quad (8)$$

The detailed expressions for e_n^f , h_n^f , \dots , h_q^g are omitted. The above equations include $5(6N + 1) + 3Q$ unknowns coefficients. The boundary conditions for the wave functions are

$$\left. \begin{aligned} \frac{E_N^f}{H_N^f}(\varphi_0^{(u)} + \varphi) &= \frac{E_N^{d-}}{H_N^{d-}}(\varphi_0^{(u)} + \varphi), & \frac{E_N^{d+}}{H_N^{d+}}(\varphi_0^{(u)} + \varphi) &= \frac{E_N^{a-}}{H_N^{a-}}(\varphi_0^{(u)} + \varphi) \\ \frac{E_N^{a+}}{H_N^{a+}}(\varphi_0^{(u)} + \varphi) &= \frac{E_Q^{g(u)}}{H_Q^{g(u)}}(\varphi_0^{(u)} + \varphi) + \frac{e^i}{h^i}(\varphi) \delta_{u0} \end{aligned} \right\} \begin{aligned} (u = 0, 1, 2; \\ -\frac{\pi}{3} < \varphi < \frac{\pi}{3}) \end{aligned} \quad (9)$$

where $\frac{e^i}{h^i}(\varphi) = \frac{E_z^i}{\zeta_0 H_z^i} \Big|_{r=a/\sqrt{3}}$ and δ_{u0} is Kronecker's delta.

Choosing the sampling points at $\varphi = \varphi_m$ ($m = 1, 2, \dots, M$) such that $18M \geq 30N + 3Q + 5$, we have the simultaneous linear equations that must be solved in the least squares sense [7].

To save the memory and CPU time, we decompose the wave functions into three parts, namely $p = 0, 1, 2$ (p : phase number), and get three independent equation sets of the reduced size as

$$\begin{pmatrix} \begin{bmatrix} e_{3\nu+p,m}^f \\ h_{3\nu+p,m}^f \\ [0] \\ [0] \\ [0] \\ [0] \end{bmatrix} & \begin{bmatrix} -e_{3\nu+p,m}^{d1} \\ -h_{3\nu+p,m}^{d1} \\ e_{3\nu+p,m}^{d3} \\ h_{3\nu+p,m}^{d3} \\ [0] \\ [0] \end{bmatrix} & \begin{bmatrix} -e_{3\nu+p,m}^{d2} \\ -h_{3\nu+p,m}^{d2} \\ e_{3\nu+p,m}^{d4} \\ h_{3\nu+p,m}^{d4} \\ [0] \\ [0] \end{bmatrix} & \begin{bmatrix} [0] \\ [0] \\ -e_{3\nu+p,m}^{a1} \\ -h_{3\nu+p,m}^{a1} \\ e_{3\nu+p,m}^{a3} \\ h_{3\nu+p,m}^{a3} \end{bmatrix} & \begin{bmatrix} [0] \\ [0] \\ -e_{3\nu+p,m}^{a2} \\ -h_{3\nu+p,m}^{a2} \\ e_{3\nu+p,m}^{a4} \\ h_{3\nu+p,m}^{a4} \end{bmatrix} & \begin{bmatrix} [0] \\ [0] \\ [0] \\ [0] \\ -e_{q,m}^g \\ -h_{q,m}^g \end{bmatrix} \end{pmatrix} \begin{pmatrix} [A_{3\nu+p}] \\ [F_{3\nu+p}] \\ [G_{3\nu+p}] \\ [C_{3\nu+p}] \\ [D_{3\nu+p}] \\ [\tilde{B}_q^{(p)}] \end{pmatrix} \\ = \begin{pmatrix} [0] & [0] & [0] & [0] & [e_m^i/3] & [h_m^i/3] \end{pmatrix}^T \quad (10)$$

where the submatrices $[e_{3\nu+p,m}^f]$, $[-e_{q,m}^g]$, $[e_m^i/3]$, for example, are composed of the elements $e_{3\nu+p}^f(\varphi_m)$, $-e_q^g(\varphi_m)$, $e^i(\varphi_m)/3$. The suffixes extend as $-N \leq \nu \leq N' = \begin{cases} N & (\text{if } p = 0) \\ N - 1 & (\text{if } p = 1, 2) \end{cases}$, $1 \leq q \leq Q$, and $1 \leq m \leq M$, so that the number of equations is $6M$ whereas the number of unknowns is $5(N + N' + 1) + Q$. The amplitude of the TE_{q0} mode was transformed by

$$\begin{pmatrix} \tilde{B}_q^{(0)} \\ \tilde{B}_q^{(1)} \\ \tilde{B}_q^{(2)} \end{pmatrix} = \frac{1}{3} \begin{pmatrix} 1 & 1 & 1 \\ 1 & \alpha^2 & \alpha \\ 1 & \alpha & \alpha^2 \end{pmatrix} \begin{pmatrix} B_q^{(0)} \\ B_q^{(1)} \\ B_q^{(2)} \end{pmatrix} \quad (11) \quad \left| \begin{array}{l} \text{with } \alpha = e^{j2\pi/3}. \text{ Equation (10) is} \\ \text{solved by the QR algorithm based on} \\ \text{the orthogonal decomposition method.} \end{array} \right.$$

4. NUMERICAL RESULTS

Figure 2 shows the cross sections of cylindrical ferrite and dielectric materials. As the number of terms included in the function $\tau_L(\phi)$ is increased, the shape approaches an equilateral triangle.

Figure 3 shows the dependence of the energy error on the truncation number N under the condition that $Q = 2N$ and $M = 2Q + 1$. The convergence becomes poor as the cross section is deformed from a circle. However the energy error for $L = 3$ goes below 1 % if $N \geq 17$.

Figure 4 shows the circulation property around the center frequency 10 GHz. In the left upper figure (a), the insertion loss ($-20 \log |B_1^{(2)}|$) is decreased when the cross section of the ferrite is deformed from a circle to a triangle. We have little difference between the curves for $L = 2, 3$. The left lower figure (b) tells us that the dielectric coating of quasi-triangular shape further decreases the loss. In the right figure (c), we add the reflection and isolation losses defined by $-20 \log |B_1^{(0)}|$ and $-20 \log |B_1^{(1)}|$, respectively. The solid curves without dielectric coating agree well with the result by the finite element method [4].

5. CONCLUSION

The Y-junction circulator of a rectangular waveguides have been analyzed by the mode matching method. After the numerical convergence is verified, The reflection, insertion, and isolation losses were computed for several cross sections of the ferrite cylinders. It was demonstrated that the introduction of the dielectric coating makes the frequency band wider.

References

1. J. B. Davies, *IRE Trans. Microwave Theory Tech.*, **MTT-10**, 596–604, 1962.
2. J. B. Castillo, Jr. and L. E. Davies, *IEEE Trans. Microwave Theory Tech.*, **MTT-18**, 25–34, 1970.
3. Y. Akaiwa, *IEEE Trans. Microwave Theory Tech.*, **MTT-22**, 954–959, 1974.
4. M. Koshiba and M. Suzuki, *IEEE Trans. Microwave Theory Tech.*, **MTT-34**, 103–109, 1986.
5. J. Abdounour and L. Marchildon, *IEEE Trans. Microwave Theory Tech.*, **MTT-42**, 1038–1045, 1994.
6. J. Helszajn, *Waveguide Junction Circulators*, John Wiley & Sons, Chichester, 1998.
7. Y. Okuno, The mode-matching method, in *Analysis Methods for Electromagnetic Wave Problems* (Chap. 4), E. Yamashita (Ed.), Artech House, Norwood, 1990.

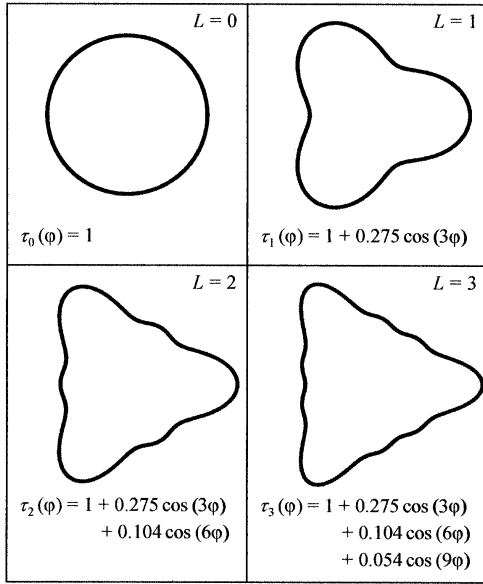


Figure 2: Cross section of the cylindrical body. Fourier coefficients of an equilateral triangle are employed.

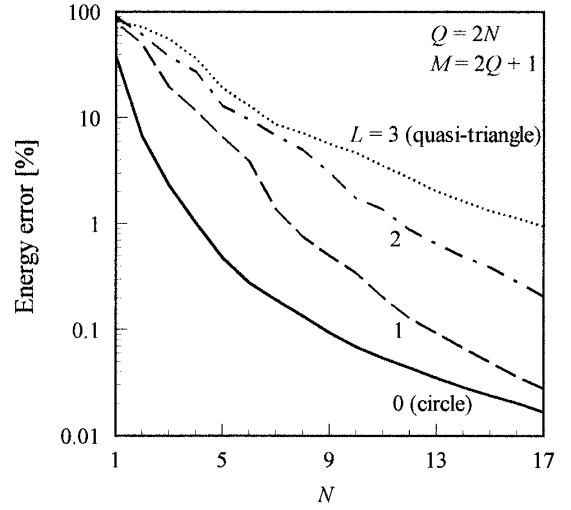
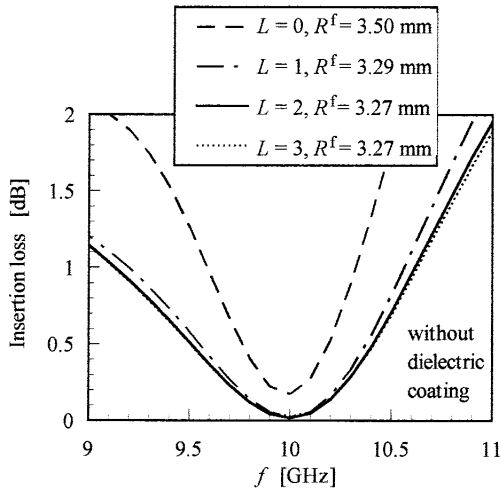
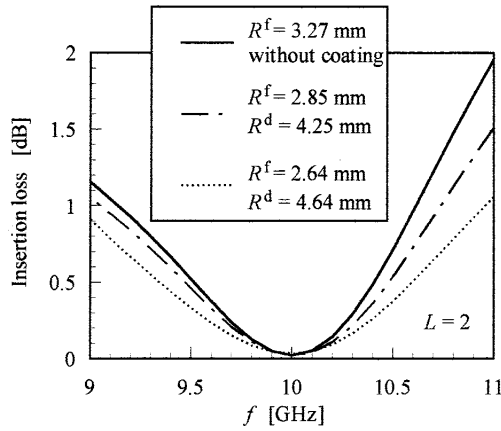


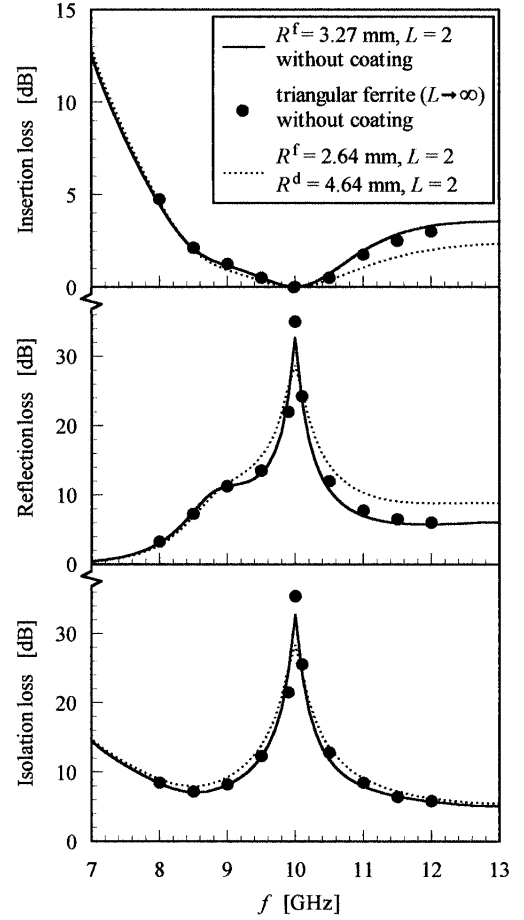
Figure 3: Energy error at $a = 22.96$ mm and $f = 10$ GHz. Ferrite parameters are $\epsilon_r = 11.7$, $M_s = 1317$ Gauss, $H_0 = 200$ Oe, and $\rho^f(\phi) = 2.66 \tau_L(\phi)$ mm. Dielectric parameters are $\epsilon_{r1} = 6.4$ (beryllia) and $\rho_L(\phi) = 3.76 \tau_L(\phi)$ mm.



(a)



(b)



(c)

Figure 4: Frequency dependence of the losses at $a = 22.96$ mm. Ferrite parameters are $\epsilon_r = 11.7$, $M_s = 1317$ Gauss, $H_0 = 200$ Oe, and $\rho^f(\phi) = R^f \tau_L(\phi)$ mm. Dielectric parameters are $\epsilon_{r1} = 3.78$ (fused quartz) and $\rho^d(\phi) = R^d \tau_L(\phi)$ mm.